

## AMORPHOUS SILICON CARBIDE HETERO-EMITTERS FOR HIGH EFFICIENCY SILICON SOLAR CELLS

S. Janz, J. Ziegler, D. Pysch, D. Suwito, S. W. Glunz  
Fraunhofer Institute for Solar Energy Systems ISE, Heidenhofstrasse 2, D-79110 Freiburg,  
Corresponding author: Stefan Janz, Tel.: +49-761-4588-5261, Fax.: +49-761-4588-9250,  
E-mail: stefan.janz@ise.fraunhofer.de

**ABSTRACT:** We investigated different amorphous  $\text{Si}_x\text{C}_{1-x}\text{:H}$  layers for their applicability as hetero-emitter materials. The deposition with Plasma Enhanced Chemical Vapour Deposition (PECVD) in a preliminary industrial stage plasma reactor was done without any wet-chemical pre-cleaning directly before the deposition. In a first step the single layers were characterised optically with Spectral Ellipsometry (SE) which showed an enhanced transparency of a- $\text{Si}_x\text{C}_{1-x}\text{:H}$  layers with a very low carbon content below 10 % compared to a-Si:H. On both sides passivated Si float zone wafers we measured minority carrier lifetimes with the Quasi Steady-State Photoconductance (QSS-PC) method which showed excellent passivation performance for 70 nm thick layers and a detrimental performance loss for thicknesses below 10 nm. With the Constant Photocurrent Method (CPM) we found a significant increase of the Urbach energy when incorporating phosphorous into the layer network. The solar cell had a hetero-junction on the front-side and a passivated rear-side ( $\text{SiO}_2$ ) with local contacts (PERC). The first cell batches were strongly influenced by technological problems such as material inhomogeneities over the cell area, contaminations on the surface and a poor grid finger/ITO adhesion behaviour. Nevertheless, we could achieve an excellent open circuit voltage of 674 mV.

Keywords: Silicon Carbide, Hetero-Junction, High-Efficiency

### 1 INTRODUCTION

Photon absorption in the emitter layer of a hetero-junction solar cell leads to a significant current loss due to cutting down of the solar spectrum of the incident light and due to enhanced recombination in the amorphous emitter layer. Furthermore, the full potential of such emitter layers, e.g. the low process temperatures, can only be attained if the c-Si/emitter interface shows low recombination activity. This leads in most cases to the necessity of a second, intrinsic layer which has to reduce the number of defects at the interface. These two layers together which form the emitter of the solar cell have most commonly been realised with amorphous, hydrogenated silicon (a-Si:H), a material which has the clear disadvantage of a fairly high absorption coefficient in the short wavelength region. As an alternative layer with excellent passivation quality, comparable mobilities and higher transparency we use amorphous, hydrogenated silicon carbide (a- $\text{Si}_x\text{C}_{1-x}\text{:H}$ ). We show optical and electrical data of these layers and their excellent passivation performance. Furthermore, first solar cells with a- $\text{Si}_x\text{C}_{1-x}\text{:H}$  hetero-emitter and a passivated rear-side will be presented.

### 2 EXPERIMENTAL DETAILS

#### 2.1 Amorphous $\text{Si}_x\text{C}_{1-x}\text{:H}$ layer deposition

As the native oxide qualities of wafers out-of-the-box show a wide range of variation we did an HNF cleaning the day before the layer depositions took place. We deposited a- $\text{Si}_x\text{C}_{1-x}\text{:H}$  layers with the precursor gases silane ( $\text{SiH}_4$ ) and methane ( $\text{CH}_4$ ) by Plasma Enhanced Chemical Vapour Deposition (PECVD) in a two source plasma reactor. This lab-type-reactor called AK400M from Roth&Rau is used at our institute to investigate new processes before transferring them to a standard industrial plasma reactor. To achieve optimum surface conditions a preceding cleaning procedure with hydrogen and argon was applied to the Si float-zone (FZ) wafer.

This in-situ pre-cleaning step made a wet-chemical cleaning procedure unnecessary. The aim of this procedure was to remove the native oxide and to saturate the dangling bonds with hydrogen atoms. Directly afterwards the a- $\text{Si}_x\text{C}_{1-x}\text{:H}$  layer was deposited. During some deposition procedures additional phosphine ( $\text{PH}_3$ ) was introduced into the chamber with flow-rates from 10 to 85 sccm to achieve phosphorous doping of the layers. The deposition time was chosen between 1 and 10 min.

#### 2.2 Layer characterisation

The determination of the optical parameters of a- $\text{Si}_x\text{C}_{1-x}\text{:H}$  was done by measurements with Spectral Ellipsometry (SE) with a M-2000F<sup>TM</sup> from the company Woolam and subsequent fitting of data with a Tauc-Lorenz-model [1]. The ellipsometry data was also used to determine the layer thicknesses. To double-check this parameter we created accurate layer interceptions and measured these structures with a mechanical profiler from the company TENCOR. In previous experiments with phosphorous doped a- $\text{Si}_x\text{C}_{1-x}\text{:H}$ -layers we observed a strong dependence of passivation performance on layer thickness [2]. As the intrinsic buffer and the emitter layers need to be as thin as possible to guarantee an optimum blue response of the solar cells we investigated this behaviour for intrinsic layers. Therefore we prepared lifetime samples by using Si float-zone (FZ) wafers <100> passivated on both-side with layers showing thicknesses ranging from 5 to 70 nm. The effective excess carrier lifetime of the passivated samples in the injection regime  $10^{14}$ - $10^{17}$   $\text{cm}^{-3}$  was determined with a WCT-120 photoconductance tool from Sinton Consulting Inc. in the transient and quasi steady-state (QSS-PC) mode [3]. As the defect concentration in a-Si:H layers in the subbandgap is known to increase with doping level (phosphorous incorporation) we characterised our layers with the Constant Photocurrent Method (CPM) [4] in order to verify such a behaviour for a- $\text{Si}_x\text{C}_{1-x}\text{:H}$ . The details of the set up can be found in reference [5].

## 2.2 Solar cell processing

Although the full potential of hetero-emitters can only be realised on n-type Si bulk material due to the higher minority carrier lifetimes, we realised our first hetero-junction solar cells on 1  $\Omega$ cm p-type FZ silicon <100>. For the amorphous emitter we chose different  $\text{Si}_x\text{C}_{1-x}\text{:H}$  layer combinations (intrinsic/n-doped) with varying thicknesses and doping concentrations. The electrically conductive window layer was indium tin oxide (ITO) deposited in a sputter reactor. As we do not have such a reactor, this process had to be farmed out. This lack of in-house-experience with ITO led to several problems in connection with metal contact formation and temperature treatment of the structures. The front grid consisted of directly evaporated Cr/Ag with a subsequent electroplating (50 nm/6-8  $\mu\text{m}$ ). The solar cells had no textured front-side. The rear-side had a full area thermal oxide passivation which was locally opened with HF (photoresist masking) and evaporated subsequently with 2  $\mu\text{m}$  of aluminium (see Figure 1). As the processing until this stage was done on 4" wafers we cut out 2x2 cm<sup>2</sup> solar cells to define the illuminated areas and to prevent a parallel connection over the on the whole area deposited ITO layer. To establish reasonable metal/semiconductor contacts, different annealing steps at temperatures between 250°C to 350°C for up to 30 min were applied.

The solar cells were characterised with the SunsVoc method [6] to measure open-circuit voltages  $V_{oc}$  without being limited by series resistance problems (e.g. without front-grid), electroluminescence [7] to identify technological processing problems and further standard methods like  $I/U$ -measurements [8].

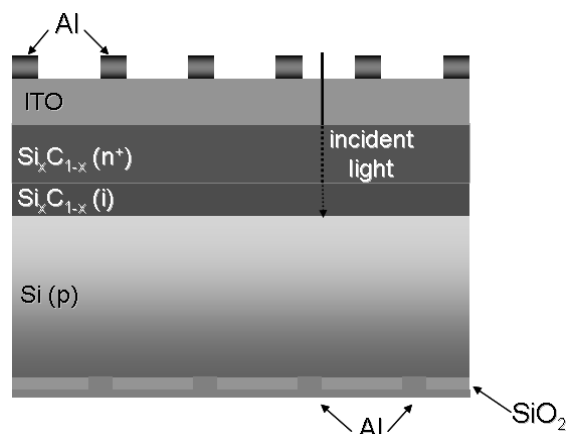


**Figure 1:** Solar cell structure of the one side hetero-structure solar cell with a dielectrically passivated (thermal  $\text{SiO}_2$ ) and locally contacted rear-side (PERC structure).

## 3 RESULTS AND DISCUSSION

In a first step amorphous  $\text{Si}_x\text{C}_{1-x}\text{:H}$  single layers were characterised optically and electrically to determine their applicability as amorphous emitter layers. Selected layers were applied afterwards as buffer and emitter on high efficiency solar cell structures.

### 3.1 Single layer and stack characterisation

In Figure 2 one can clearly see from the spectral

ellipsometry measurements an improved transparency of the  $\text{a-Si}_x\text{C}_{1-x}\text{:H}$  layer compared to an  $\text{a-Si:H}$  layer. The reference data for the  $\text{a-Si:H}$  layer come from the Woolam-database. This behaviour can be explained by the incorporation of carbon in the layer's network which leads to a widening of the optical band gap [9].

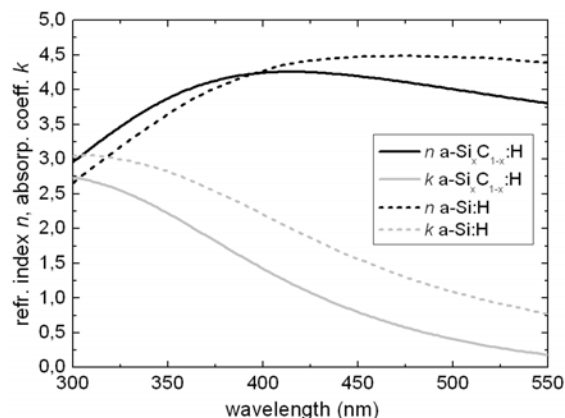


**Figure 2:** Optical parameters  $n$  (black) and  $k$  (gray) measured with spectral ellipsometry (SE) for  $\text{a-Si}_x\text{C}_{1-x}\text{:H}$  (solid) and  $\text{a-Si:H}$  (dotted) layers.

Though an introduction of additional defects coming from unsaturated carbon bonds can be expected, photoconductivity measurements reveal a still excellent passivation performance for such layers (see Figure 3). Possible reasons could be the high amount of hydrogen to overcome this negative effect or only a moderate increase in defect density. We can conclude from these measurements that even a relatively low amount of carbon (around 10%) leads to layers which have a much higher transparency (see Figure 2) without suffering in the electrical quality.

The thickness dependence of the passivation performance (intrinsic  $\text{Si}_x\text{C}_{1-x}\text{:H}$ ) can also be found in Figure 3. Below 70 nm of layer thickness the shape seems to follow a logarithmic function whereas below 10 nm this function decreases dramatically which is well known for  $\text{a-Si}_x\text{C}_{1-x}\text{:H}$  deposited with a parallel plate reactor [10] and for  $\text{a-Si:H}$  layers as well.

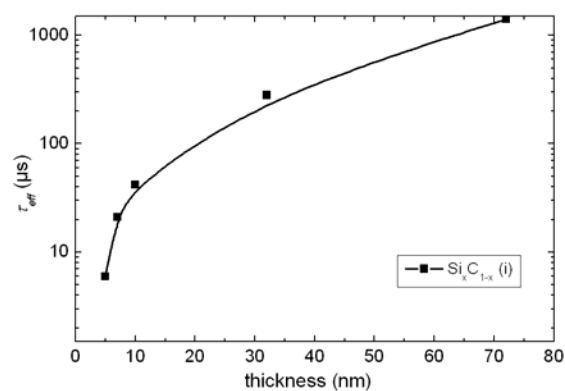


**Figure 3:** Quasi-Steady-State Photoconductance (QSS-PC) measurements of 1  $\Omega$ cm FZ Si wafers passivated on both sides with intrinsic  $\text{a-Si}_x\text{C}_{1-x}\text{:H}$  layers with thicknesses ranging from 5 to 70 nm.

The still increasing passivation performance with thicknesses above 30 nm is surprising in the first place

because the passivation effect should be dominated by saturation of defects at the interface. Nevertheless a second process could possibly be having a strong influence on the thickness/passivation behaviour of our layers. As the deposition time increases with layer thickness, a diffusion of hydrogen atoms to the c-Si/a-Si<sub>x</sub>C<sub>1-x</sub>:H interface (in-situ hydrogenation) takes place which could further enhance the passivation performance. In any case, it is clear that a maximum possible thickness of the amorphous layer is desirable in terms of passivation quality, but additional hydrogen passivation without any layer thickening could play another key role as well. Upcoming experiments shall give further evidence of such behaviour.

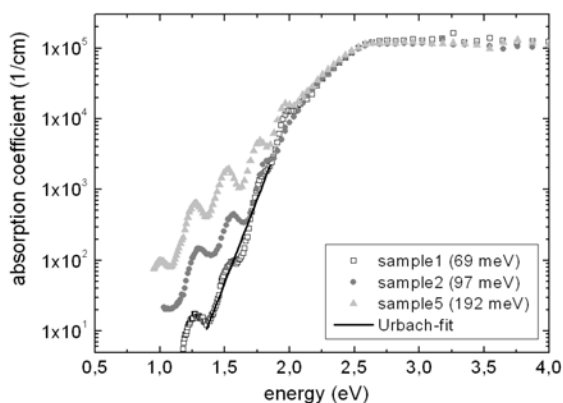


**Figure 4:** Constant Photocurrent Method (CPM) measurements of three a-Si<sub>x</sub>C<sub>1-x</sub>:H-layers deposited with no additional (sample 1), with 10 sccm (sample 2) and 40 sccm (sample 5) PH<sub>3</sub> flow during deposition.

The emitter layer itself has to be doped with phosphorous to form a p/n-junction and to achieve a sufficiently high electrical conductivity. This incorporation of phosphorous atoms into the layer's network leads to an increase of defect densities which can be measured quantitatively as an increase of the Urbach energy. In Figure 4 one can find the CPM measurements and the corresponding Urbach-fits of three Si<sub>x</sub>C<sub>1-x</sub>:H layers with different doping levels. Interference effects due to inappropriate layer thicknesses make an accurate fit very difficult but the tendency of increasing Urbach energies by the factor of three from intrinsic (69 meV) to "normally" doped (192 meV) layers is nevertheless significant. This higher number of subbandgap defect states in the emitter layer limits solar cells without any intrinsic buffer layers. But also very thin intrinsic buffer layers do not automatically prevent an enhanced recombination of minority carriers in the doped amorphous layer (smearing wave function) [11].

### 3.2 Solar cell results

In the first solar cell batches with a-Si<sub>x</sub>C<sub>1-x</sub>:H hetero-emitters some technological problems occurred which showed a detrimental impact on our solar cell results and made it difficult to extract information concerning the emitter itself. The electroluminescence measurements presented in Figure 5 point out some technological problems. In comparison to the successfully processed solar cell (top left) contaminations and structural defects at the c-Si surface such as tweezers prints (bottom left) can be observed. Other samples show blistering effects of

the emitter layer (top right) and shunting (bottom right). The electroluminescence of a large number of solar cells leads to the conclusion that such technological errors occurred only on occasion and can be prevented in most cases.

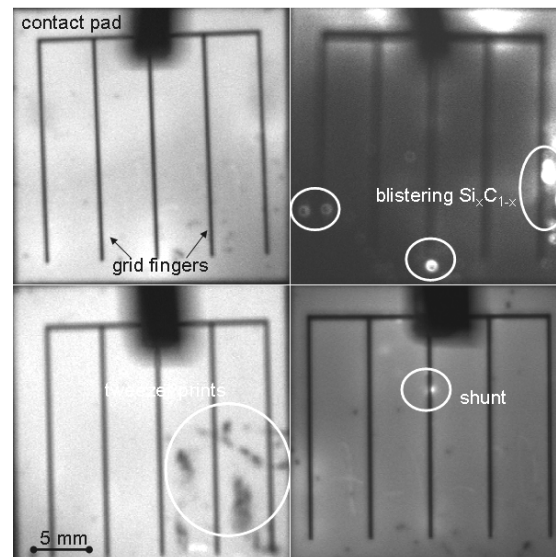


**Figure 5:** Electroluminescence of 4 different hetero solar cells with technological errors such as blistering of the a-Si<sub>x</sub>C<sub>1-x</sub>:H layers (top right), tweezers prints on the Si wafer (bottom left) and shunts below the grid fingers (bottom right).

All solar cells were measured with SunsVoc without a front-grid and before separation (7 cells on each 4" wafer). As shown in Figure 6, the scatter of the measured  $V_{oc}$  values on the same wafer is quite high. Especially for the cells with a 12 nm emitter single layer (grey squares) we measured voltages ranging between 473 and 535 mV. Possible reasons are process inhomogeneities over the wafer area (see Figure 5) or the still undefined solar cell area. We can nevertheless draw some conclusions which are as follows: The 20 nm thick emitter single layer (grey triangles) seems to be superior to the 12 nm emitters over the whole doping range. When applying a layer stack of 12 nm intrinsic and 16 nm highly doped a-Si<sub>x</sub>C<sub>1-x</sub>:H the  $V_{oc}$  reaches even higher values of up to 666 mV.

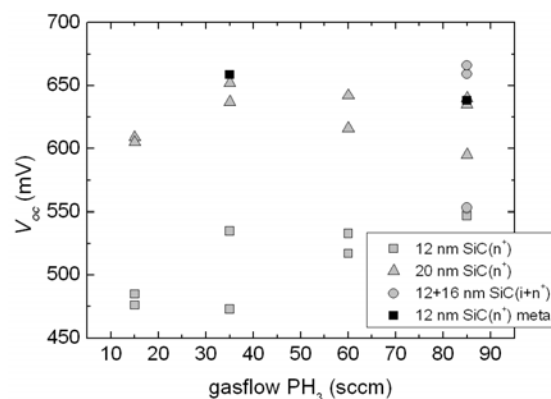


**Figure 6:** SunsVoc measurement of solar cells before (grey) and after (black) front-grid evaporation and electroplating.

In a next step the front-grid was defined with photolithography, evaporated and electroplated. Afterwards the single solar cells were cut out of the wafer with a chip saw. Unfortunately the adhesion of the metal fingers was very poor for a lot of cells. Therefore we had to repeat the evaporation and the electroplating process which did not lead to satisfying results in all cases. Individual SunsVoc measurements on the 2x2 cm<sup>2</sup> cells with front-grid showed that  $V_{oc}$  values are still better compared to measurements on the whole wafer. In Figure 6 two examples of single layer emitters with two different doping levels are shown. For these samples an improvement on the separated cells of more than 100 mV was measured. This gives us great confidence for the solar cells which could not be finished yet due to the troubles with grid finger deposition stated above.

**Table I:** Solar cell results for a single one side hetero-structure cell with a passivated rear-side without and with additional annealing (2x2 cm<sup>2</sup>).

annealing	$V_{oc}$ (mV)	$J_{sc}$ (mA/cm <sup>2</sup> )	$FF$ (%)	$\eta$ (%)
No annealing	530	31.9	61.6	10.4
Temp. low	644	31.8	73.5	15.0
Temp. high	674	31.5	66.7	14.1

First solar cell results for a single cell are shown in Table 1. This cell has a highly doped single a-Si<sub>x</sub>C<sub>1-x</sub>:H emitter with a thickness of 12 nm. Several annealing procedures pushed the  $V_{oc}$  from initial 530 mV to a maximum value of 674 mV. The fill-factor is relatively low with just 66.7 % which points to anticipated contact problems between ITO and metal grid. As this behaviour is not comprehensively investigated and understood it will be the subject of publications to come.

It is even more disappointing that the solar cells with the double layer emitter which already showed very good  $V_{oc}$  values (SunsVoc) on the wafer could not be finished so far. Nevertheless the solar cell presented here shows one of the best open circuit voltages ever reported on p-type silicon with a PERC rear structure.

#### 4 CONCLUSIONS AND OUTLOOK

The investigation of different amorphous Si<sub>x</sub>C<sub>1-x</sub>:H layers as hetero-emitter materials showed the high potential of this material for a hetero-junction application.

The single layers showed an enhanced transparency for a-Si<sub>x</sub>C<sub>1-x</sub>:H layers with very low carbon content below 10 % over a-Si:H. The passivation performance of these intrinsic layers was excellent but had a detrimental performance loss below 10 nm layer thickness. One reason could be the short deposition time which means just a short hydrogenation as well. With CPM we found a significant increase of the Urbach energy when incorporating phosphorous into the layer network. This does not necessarily interfere with the potential for a good solar cell as long as a thin intrinsic buffer layer is introduced between the c-Si wafer and the amorphous emitter layer.

The solar cell processing was strongly influenced by technological problems such as material inhomogeneities

over the cell area, contaminations on the surface and a poor grid finger/ITO adhesion behaviour. We expect a learning curve with repetitions to come. Although only few solar cells could be finished so far we achieved excellent open-circuit voltages of up to 674 mV.

Our experiences with the PECVD deposition in our preliminary industrial stage plasma reactor gives us confidence that the process transfer to a large area and high throughput reactor should be possible.

#### 5 ACKNOWLEDGEMENTS

The authors would like to thank all their colleagues for valuable activities and discussions such as J. Lacombe for the CPM measurements and for the ITO deposition done in Gelsenkirchen. Furthermore M. Kasemann for the electroluminescence measurements and A. Leimenstoll, S. Seitz, C. Schetter and A. Herbolzheimer who did all major solar cell processes.

#### 6 REFERENCES

- [1] H. G. Tompkins, Academic Press (1993).
- [2] S. Janz, D. Suwito, S.W. Glunz, Proceedings of the 22nd EUPVSC, Milano, Italy (2007) pp. 1454-1457.
- [3] R. A. Sinton and A. Cuevas, Appl. Phys. Lett., 69 (1996) 2510-2.
- [4] M. Vaněček, J. Kočka, J. Stuchlik and A. Triska, Solid State Communications 39 (1981) pp. 1199-1202.
- [5] J. Lacombe (2007) Diplomarbeit, Universität Münster.
- [6] R. A. Sinton and A. Cuevas, Proceedings of the 16<sup>th</sup> EUPVSC, Glasgow, Scotland (2000).
- [7] Fuyuki, T., H. Kondo, T. Yamazaki, Y. Takahashi, and Y. Uraoka, Appl. Phys. Lett., 86 (2005) p. 262108.
- [8] A. Goetzberger *et al*, B. G. Teubner, Stuttgart, Germany (1977).
- [9] S. Janz, Verlag Dr. Hut, München (2007) ISBN 978-3-89963-563-8, pp. 53-61.
- [10] Ferre, R. Martin, I. Vetter, M. Garin, M. Alcubilla, R. Appl. Phys. Lett., 87 (2005) p. 202109.
- [11] A. Froitzheim, IEEE (2002) pp. 1238-1241.